Journal of Materials Chemistry A

Accepted Manuscript

ROYAL SOCIETY OF CHEMISTRY

www.rsc.org/materialsA

Evaluation of nanocrystalline Sn_3N_4 derived from ammonolysis of $Sn(NEt_2)_4$ as a negative electrode material for Li-ion and Na-ion batteries

Xianji Li, Andrew L. Hector*, John R. Owen and S. Imran U. Shah

Chemistry, University of Southampton, Southampton SO17 1BJ, UK. A.L.Hector@soton.ac.uk

Bulk nanocrystalline Sn_3N_4 powders were synthesised by a two step ammonolysis process followed by washing with dilute acid. Their performance as Li-ion and Na-ion battery negative electrodes was assessed by galvanostatic cycling in half cells vs the metal, giving good performance in both cases and remarkable stability in the sodium cells. The effect of carboxymethyl cellulose and sodium alginate binders was examined and the latter found to give superior performance. Capacity and stability were also enhanced *via* the use of a fluoroethylene carbonate electrolyte additive.

Introduction

Interest in sodium-ion batteries has ramped up drastically in recent years, with <50 journal papers published in 2011 and >800 in 2015.[1] This stems from a realisation that as large scale applications of energy storage, including in transport, become more significant, the economically viable supply of lithium minerals may become price determining.[2] Graphite is the most popular negative electrode material in lithium-ion batteries, but the larger sodium ions intercalate very poorly into its layered structure.[3] Hence the literature on negative electrode materials has been dominated by amorphous "hard" carbons, alloys with elements such as Sn and Sb, and oxides.[4] Recently a number of transition metal nitrides have shown promising performance as sodium battery negatives, including work by ourselves on Ni_3N,[5] Cu_3N[6] and Mn_3N_2,[7] and by Cui *et al* on VN.[8] These operate by a conversion mechanism at the particle surfaces, with reduction of the metal nitride to the metal, presumably with amorphous sodium nitride also formed. No studies of p-block nitrides in sodium cells have yet been published.

Tin nitride, Sn_3N_4, adopts the spinel structure,[9] and was first prepared by Fischer and Iliovici using an electrical discharge method in 1909.[10] The first bulk preparation by Maya in 1991 was achieved by reaction of $SnBr_4$ with KNH_2 in liquid ammonia, followed by thermal decomposition of the resultant polymer $[Sn(\mu\text{-}NH)(NH_2)_2]_n$ with loss of ammonia to make X-ray amorphous Sn_3N_4.[11] Ammonia was evolved around 100 °C and nitrogen (with reduction of the tin) at around 400 °C. The crystal structure determination by Scotti *et al* in 1999 used a modification of this route.[9] At around the

same time as Maya's bulk synthesis, Gordon *et al* produced crystalline Sn_3N_4 thin films by chemical vapour deposition from $Sn(NMe_2)_4$ and ammonia,[12] and various other thin film preparation routes have been examined since.[13,14,15] Higher temperature synthesis was achieved by Shemkunas *et al* using a metathesis reaction between SnI_4 and Li_3N at elevated pressure,[16] although washing with $HCl_{(aq)}$ was necessary to remove by-produced tin metal.

Our current interest in Sn_3N_4 stems from a number of recent studies in sodium negatives where conversion of antimony or tin containing materials is combined with formation of alloys with sodium, with the combination of the two storage mechanisms delivering a higher capacity overall. Sb_2S_3,[17] SnS,[18,19] SnS_2,[20] Sn_4P_3[21,22,23] and SnO_2[24,25,26] have all been examined in this context, typically in recent studies in composites with graphene or carbon nanotubes to improve electronic conductivity. Following an effort by Fuji to commercialise tin oxide-containing cells, the mechanisms of lithium storage were studied in detail by Dahn.[27] It was found that the initial reduction produced lithium oxide and that reversible cycling only involved tin alloying, but that the lithium oxide matrix improved the stability of that cycling relative to tin itself. The possibility that Sn_3N_4 could deliver more capacity than other metal nitrides is clear. Two previous studies have examined Sn_3N_4 in lithium cells, and both used RF sputtered thin film samples. Park *et al* suggested that irreversible reduction to tin followed by alloying/de-alloying were the dominant mechanisms of charge storage.[28] Baggeto *et al* later found that more than 6 Li atoms per Sn atom could be stored and argued that conversion and alloying must both be working reversibly, with retention of a volumetric capacity of 700 μAh cm^{-2} μm^{-1} possible over 50 cycles and the possibility of extending this to 100 cycles if only ~80% of this capacity was utilised.[29]

Herein we produce nanocrystalline Sn_3N_4 by ammonolysis of a tin(IV) dialkylamide. We examine its suitability as a sodium-ion or lithium-ion negative electrode material in conventional half cells using composite electrodes with carbon black and a binder. We then examine the effect of addition of fluoroethylene carbonate (FEC) to the electrolyte on the cycling performance.

Experimental

Synthesis was carried out under dry nitrogen using glove box and Schlenk techniques until after the tin nitride had been fired under ammonia. $LiNEt_2$ was obtained by reacting diethylamine (50 cm^3, Aldrich, dried by distillation from BaO) with ice cold 1.6 mol dm^{-3} ^{n}BuLi solution in hexanes (500 cm^3, Aldrich), filtering and drying the white solid *in vacuo*. Diethylether, hexane and THF (Fisher) were dried by distillation from sodium/benzophenone ketyl ether.

$Sn(NEt_2)_4$ was prepared by a modification of a published procedure.[30] $LiNEt_2$ (23 g, 0.3 mol) was suspended in a mixture of diethylether (150 cm^3) and hexane (100 cm^3), stirred to dissolve and then cooled over ice. $SnCl_4$ (8.9 cm^3, 0.075 mol, Aldrich) was dissolved in hexane (50 cm^3) and added dropwise to the cold $LiEt_2$ solution. The mixture was stirred overnight at ambient temperature, then the solvent was removed *in vacuo* leaving a light brown oil. ^1H NMR ($CDCl_3$ solution, Bruker AV300) showed the expected ethyl group signals[31] (quartet at δ 3.13 and triplet at δ 1.14) and only minor impurities. Combustion analysis showed 45.5% C, 9.5% H and 11.9% N (theory 47.2% C, 9.9% H, 13.7% N). This material was used without further purification.

Synthesis of Sn_3N_4 from $Sn(NEt_2)_4$ used a two-stage ammonolysis procedure. $Sn(NEt_2)_4$ (2 cm^3) was dissolved in THF (20 cm^3) and cooled to -78 °C, then liquid ammonia (~25 cm^3) was added by distillation from a sodium/liquid ammonia solution. This solution was allowed to warm slowly to ambient temperature with stirring, over which period the excess ammonia evaporated leaving a slurry of pale yellow powder. The solid was collected by filtration and dried *in vacuo* (~1.5 g, C 10.3%, H 5.4%, N 14.2%). Portions of this xerogel were placed into an alumina boat in a silica tube with an arrangement of taps to allow all hoses to be flushed before exposing the solid to a gas flow. The solid was then heated under flowing ammonia (BOC anhydrous grade, further dried by passing through a column of 3 Å molecular sieves) at 150 °C for 6 h, followed by a ramp (2 °C min^{-1}) to 300, 350 or 400 °C and maintenance of this temperature for 2 h. The product was then washed in air with 3 mol dm^{-3} $HCl_{(aq)}$ followed by 3 portions of ethanol, and air dried.

Electrochemical testing used a Bio-Logic SP150 or MPG potentiostat. The working electrode consisted of a powdered mixture of 75% active material with 20% of acetylene black (Shawinigan, Chevron Phillips Chemical Co. LP) and 5% binder (carboxymethyl cellulose (CMC) or sodium alginate, Aldrich) suspended into deionized water to form an ink which was then dropped onto 50 µm thick, 10 mm diameter copper foil disks. Two-electrode Swagelok cells were assembled using lithium or sodium metal foil (Aldrich, 99.9%) as the counter and pseudo reference electrode. Two sheets of dried Whatman GF/D borosilicate glass fibre were used as the separator, soaked with 6 drops of electrolyte. Lithium cells were prepared with a 1 mol dm^{-3} $LiPF_6$ in ethylene carbonate/dimethyl carbonate (1:1) electrolyte (BASF). Sodium cells used a 1 mol dm^{-3} $NaPF_6$ in ethylene carbonate/diethyl carbonate (1:1) electrolyte. The electrolyte components were purified separately (solvents distilled from BaO and $NaPF_6$ dried in vacuo at 120 °C) before combining in the glove box. In some cases 5% of the solvent was replaced with FEC (Aldrich). Cells were studied under cyclic voltammetric and galvanostatic conditions.

Powder X-ray diffraction (XRD) patterns were recorded on Bruker a D2 Phaser using Cu-K_α radiation in Bragg-Brentano geometry. Rietveld refinements used the GSAS package,[32] with a LaB_6 standard used to define the Gaussian instrumental peak shape and crystallite size extracted from the Lorentzian crystallite size broadening term.[33] *Ex situ* XRD patterns of electrodes before and after electrochemical treatment were collected in grazing incidence geometry (1° incidence angle) with Cu-K_α X-rays using a Rigaku Smartlab with a DTex250 1D detector and a sealed, glove box-loaded sample holder with a thin hemi-cylindrical Kapton window. The morphology was examined by transmission electron microscopy (TEM) on a Hitachi H7000 with an accelerating voltage of 75 kV, using samples prepared by ultrasound dispersion into distilled methanol and dropping onto carbon grids. Infrared (IR) spectra were recorded on a Perkin Elmer Spectrum 100 FTIR with samples prepared as KBr discs. Surface areas were calculated using the Brunauer-Emmett-Teller (BET) method[34] with nitrogen adsorption data collected using a Gemini 2375 surface area analyser. Combustion microanalyses (C, H and N) were outsourced to Medac Ltd.

Results and Discussion

Ammonolysis reactions of metal amides are common in CVD of metal nitrides, and this has been demonstrated in production of Sn_3N_4 films. [12] Their use in bulk synthesis of nanocrystalline metal nitride powders by reaction with neat liquid ammonia was first shown by Brown and Maya,[35] but ammonolysis in hydrocarbon solutions as used here was first used by Baxter *et al*.[36] We have also used these reactions to produce a number of high oxidation state metal nitrides[37,38,39,40] and molybdenum nitride supercapacitor electrodes.[41] Metal dialkylamides are produced on kg scales as precursors for thin film formation, hence these reactions are potentially scalable for battery materials applications. Ammonolysis proceeds by transamination reactions to produce bridging imide groups, and with $Sn(NEt_2)_4$ it is expected that they would take the form:

$$n\,\mathrm{Sn(NEt_2)_4} + nxy\,\mathrm{NH_3} \rightarrow \left[\mathrm{Sn(\mu-NH)}_x\mathrm{(NH_2)}_y\mathrm{(NEt_2)}_z\right]_n + (4-z)n\,\mathrm{HNEt_2}$$

The combustion analysis given in the experimental suggests ~0.7 NEt_2 groups per tin atom remain in our tin imide polymers. Further ammonolysis of the polymers at elevated temperature is necessary to achieve decomposition to a metal nitride, and where this is carried out under ammonia further transamination is possible as well as condensation. Hence it can be effective in removal of residual carbon.[37] Ammonolysis at 300 °C resulted in an X-ray amorphous or poorly crystalline material (Fig. 1) with an infrared spectrum showing broad ν(N-H) bands at 3200 and 3400 cm^{-1} merging with ν(C-H) at ~2800 cm^{-1}, δ(NH_2) at 1609 cm^{-1} and a strong ν(N-H) band at 550 cm^{-1} (supplementary information). The surface area of this sample (BET) was 9 $m^2\,g^{-1}$.

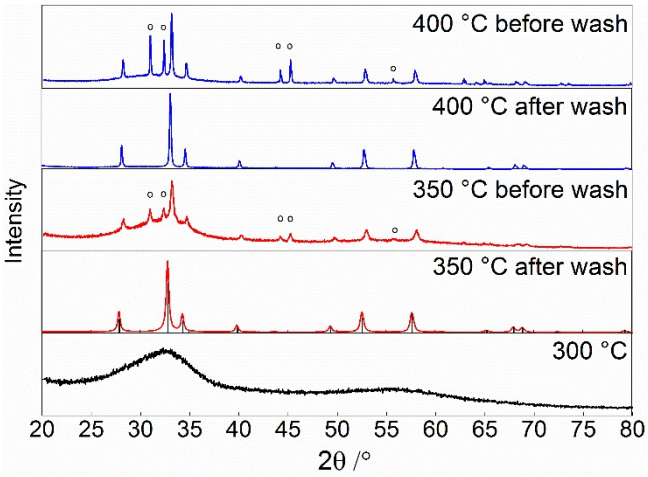

Fig. 1 Powder XRD patterns of the products of ammonolysis of the tin imide polymers at various temperatures, and after washing with $HCl_{(aq)}$. Open circles mark the positions of reflections due to tin metal, and the stick pattern on the 350 °C after washing pattern is that of Sn_3N_4.[9]

Ammonolysis of the tin imide polymer at 350 or 400 °C resulted in crystallisation of Sn_3N_4 with by-produced tin metal (Fig. 1). This is in line with a previous high pressure synthesis[16] and the remedy used there of washing with dilute HCl was also successful here in producing single phase Sn_3N_4. Interestingly the sample produced at 350 °C and HCl washed material had a high surface area of 40 $m^2\ g^{-1}$, whereas the same procedure at 400 °C only gave 9 $m^2\ g^{-1}$. The crystallites are smaller at 350 °C (broader XRD peaks) than at 400 °C, and the extra surface area in the 350 °C sample relative to the amorphous material may be due to removal of some aggregation or opening of pores when tin is washed away. The 350 °C material was the most interesting for batteries due to its higher surface area, so was carried forward for further study. A Rietveld fit to the XRD pattern of this material (R_{wp} = 3.6%, R_p = 2.8%, supplementary information) produced a lattice parameter of 9.03716(5) Å, matching Scotti's neutron diffraction value of 9.037(3) Å,[9] and an average crystallite size of 32(2) nm. TEM shows crystallites of around this size with limited aggregation (Fig. 2).

Electrochemical behaviour of Sn_3N_4 in sodium half cells

Polyvinylidene fluoride is usually the binder of choice in producing composite electrodes for lithium ion cells, but it tends to crack during cycling of alloying and conversion electrodes due to the large volume changes that occur as a result of these processes. Carboxymethyl cellulose (CMC) has exhibited a good ability to withstand these large volume changes in cycling of Si,[42] Sn[43] and Fe_2O_3,[44] providing improved performance in these cell types. CMC works best if composite electrodes are assembled from aqueous inks, and a previous attempt to use this binder with a metal nitride resulted in conversion to the oxide.[6] Recently sodium alginate, another binder applied in aqueous inks, showed even better performance than CMC in lithium cells using Si[45] or Fe_2O_3[46] as negative

electrode materials. Sn_3N_4 has good stability in deionised water, so initially electrodes using CMC and sodium alginate were compared. The aqueous Sn_3N_4/acetylene black/binder inks were dropped onto copper foil and these composite electrodes were used to assemble standard sodium half cells with a sodium counter electrode, glass fibre separator and $NaPF_6$/EC/DEC electrolyte.

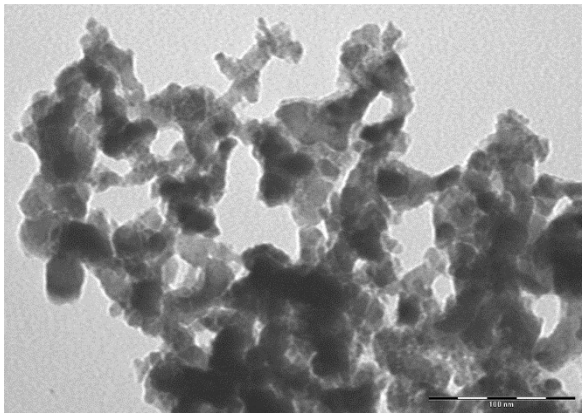

Fig. 2 TEM image (scale bar = 100 nm) of Sn_3N_4 produced by ammonolysis of the tin imide polymer at 350 °C followed by washing with dilute HCl.

The theoretical capacity of a Sn_3N_4 electrode is based on complete conversion to tin metal and alloying to the maximum sodium content:

$$Sn_3N_4 + 12Na^+ + 12e^- \rightarrow 4Na_3N + 3Sn$$

$$4Sn + 15Na^+ + 15e^- \rightarrow Na_{15}Sn_4$$

These equations predict a combined capacity of 1440 mA h g^{-1}, but using this method to calculate "C-rates" (1C represents a current designed to fully charge or discharge the cell in one hour) is unreliable as the extent of the processes that can be achieved is unknown. Instead specific currents will be quoted herein, but consider that based on the above equations a current of 100 mA g^{-1} is equivalent to a C-rate of C/14.4.

In galvanostatic cycling of Sn_3N_4 electrodes prepared with a CMC binder (supplementary information) *vs* Na at 100 mA g^{-1}, 420 mA h g^{-1} charge was passed in the first reduction and 157 mA h g^{-1} of this was recovered in the first oxidation to 3 V. This low Coulombic efficiency in the first cycle (37%) is common in conversion materials and is due to irreversible processes including the formation of interface layers. In the lithium reduction of SnO_2 the irreversible formation of Li_2O is a significant contributor to low first cycle efficiency,[27] and low first cycle efficiencies are also seen in the existing studies of SnO_2-carbon composites in sodium cells.[24,25,26] Capacity was maintained very well in subsequent cycles, with 150 mA h g^{-1} passed in the 50th oxidation, 96% of the first oxidation value. At 200 mA g^{-1} a similarly flat profile was obtained, with 118 mA h g^{-1} in the first oxidation and 110

mA g^{-1} in the 50th. Despite this good performance with a CMC binder, the better performance with sodium alginate (next paragraph) led to discontinuation of the work with CMC.

The galvanostatic performance of Sn_3N_4-sodium half-cells prepared using a sodium alginate binder was investigated at 200 mA g^{-1} for 50 cycles and 50 mA g^{-1} for 100 cycles. As with the cells using CMC binders, a low Coulombic efficiency was found in the first cycle but stable cycling followed (Fig. 3). 538 mA h g^{-1} of charge was passed in the first reduction at 200 mA g^{-1} and 118 mA h g^{-1} (22%) of this charge was recovered on reoxidation, while 705 mA h g^{-1} was passed during reduction at 50 mA g^{-1} of which 198 mA h g^{-1} (28%) was recovered during the oxidation. In the 50th cycle at 200 mA g^{-1} the oxidation capacity was 152 mA h g^{-1}, 129% of the first oxidation capacity. In the 100th cycle at 50 mA g^{-1} 188 mA h g^{-1} was passed on oxidation, 95% capacity retention. This excellent cycling capability is combined with charge/discharge profiles in which a high proportion of the capacity is utilised below 2 V making these good negative electrode materials. It is also noteworthy that based on the reversible capacity the C-rate at 200 mA g^{-1} is around 1.3, so the good cycling performance is based on a relatively high charge/discharge rate.

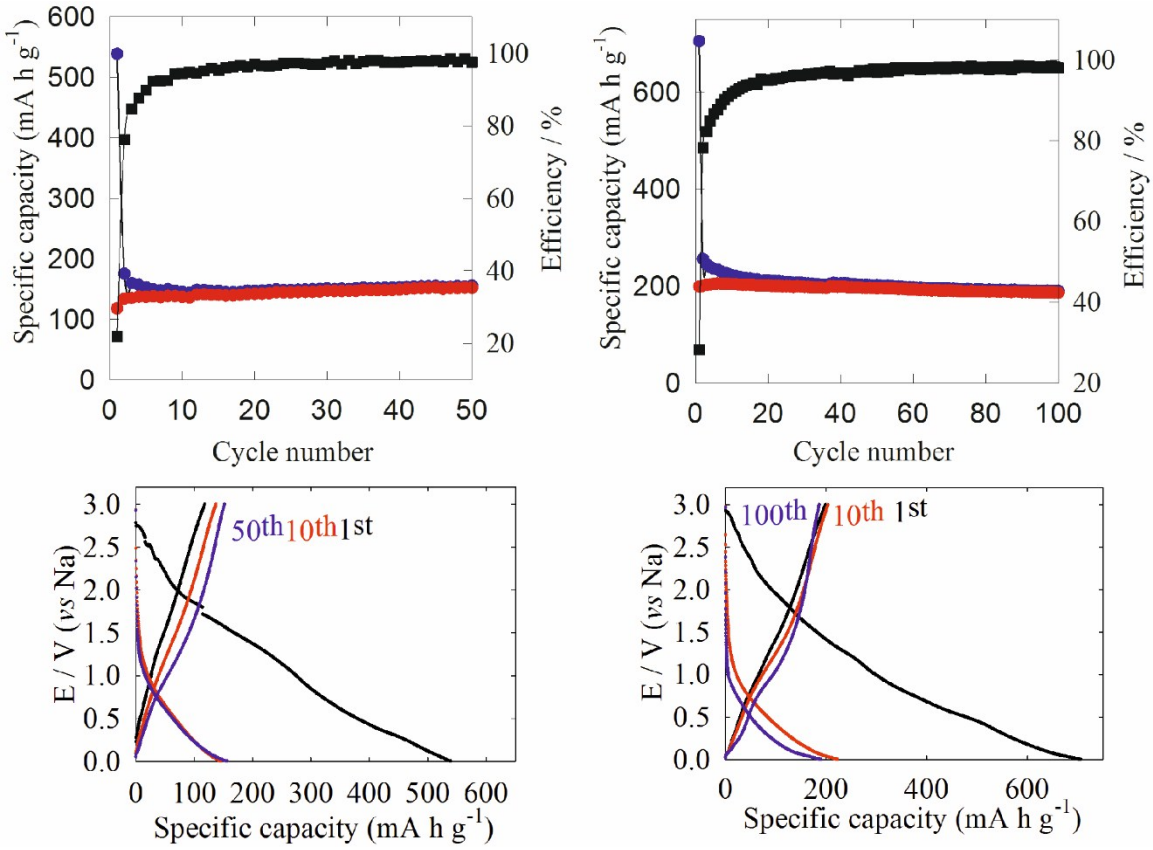

Fig. 3 Specific capacity versus cycle number (top, reduction blue, oxidation red and Coulombic efficiency black) and voltage profile against specific capacity (bottom), of Sn_3N_4/sodium half cells made with sodium alginate binder, cycled between 1 mV and 3 V for 50 cycles at 200 mA g^{-1} (left) or for 100 cycles at 50 mA g^{-1} (right).

The rate capability Sn_3N_4 in sodium half-cells was explored by cycling a cell sequentially at various current rates between 50 and 400 mA g^{-1}, Fig. 4. The Sn_3N_4 electrode offered an average reversible capacity of around 216 mA h g^{-1} in the first 10 cycles at 50 mA g^{-1}, 190 mA h g^{-1} in the next 10 cycles at 100 mA g^{-1}, 164 mA h g^{-1} at 200 mA g^{-1}, 127 mA h g^{-1} at 400 mA g^{-1} and 220 mA h g^{-1} in the final set of cycles at 50 mA g^{-1}. It is interesting to note that the reversible reduction capacity at 400 mA g^{-1} is around 55% of the capacity in the first 10 cycles at 50 mA g^{-1}, and that the capacity in the final set of cycles at 50 mA g^{-1} is actually slightly higher than that of the new electrode in the first few cycles. These results also show that Sn_3N_4 with sodium alginate binder has good cycle stability in these sodium cells even when used at multiple rates.

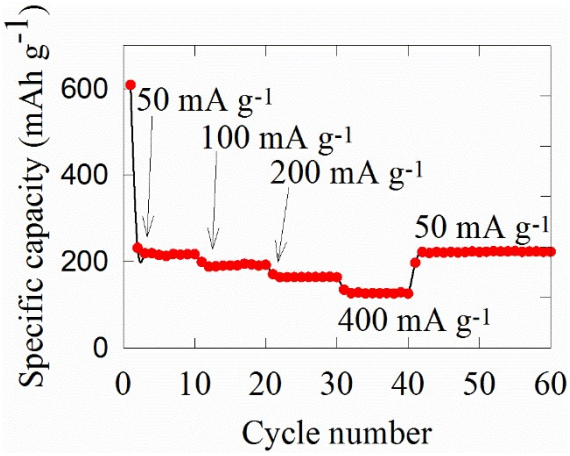

Fig. 4 Reduction specific capacity of Sn_3N_4 with sodium alginate binder in a sodium half-cell at various sequential current rates from 50 to 400 mA g^{-1} over 60 cycles.

In order to understand the charge storage mechanism of Sn_3N_4 in sodium cells, *ex situ* XRD experiments were conducted and the patterns are shown in Fig. 5. All patterns of cycled cells show several minor peaks below 28° due to residual electrolyte at the electrode surface.[21] Whilst no other new reflections are observed during cycling, after the first reduction to 1 mV the intensity of Sn_3N_4 reflections had decreased significantly relative to the copper substrate peaks, suggesting partial conversion of Sn_3N_4 to amorphous compounds. The broad feature in the background which grows in near to 20° closely resembles that observed by Kim *et al* on reduction of tin phosphide in sodium cells and attributed to an amorphous Na-Sn alloy.[21] On re-oxidation, the intensity of the broad background feature diminished and the Sn_3N_4 peaks regained some intensity relative to the copper, suggesting that Sn_3N_4 was regenerated and explaining the good cycling behaviour of this phase. In the second reduction, the intensity of Sn_3N_4 reflections again became weaker relative to copper.

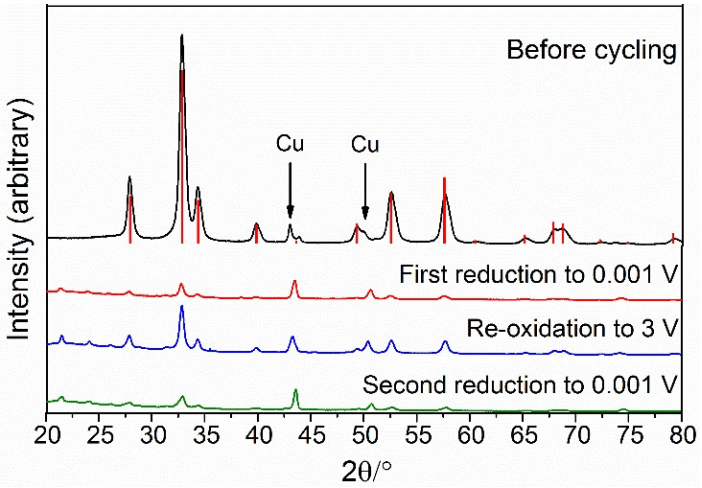

Fig. 5 *Ex situ* XRD of Sn_3N_4 electrodes cycled at 50 mA g^{-1} to different stages in sodium half cells. The red stick pattern denotes the literature positions and intensities of Sn_3N_4 reflections,[9] and the main copper substrate peaks are labelled.[47]

Electrochemical behaviour of Sn_3N_4 in lithium half cells

The electrochemical performance of Sn_3N_4 electrodes lithium cells has only previously been investigated using samples in thin film form.[28,29] Hence, the Sn_3N_4/acetylene black/sodium alginate electrodes described above were also examined in lithium half cells with a standard $LiPF_6$/EC/DMC electrolyte. As in the sodium cells reduction and alloying could be envisaged as shown in the following equations, based on which the theoretical capacity is 1560 mA h g^{-1} and charge/discharge at 100 mA g^{-1} is equivalent to a C-rate of C/15.6.

$$Sn_3N_4 + 12Li^+ + 12e^- \rightarrow 4Li_3N + 3Sn$$

$$Sn + 4.4Li^+ + 4.4e^- \rightarrow Li_{4.4}Sn$$

In galvanostatic cycling, 1550 mA h g^{-1} charge was passed in the first reduction of Sn_3N_4 at 200 mA g^{-1} (Fig. 6). However an even higher reduction capacity of 2600 mA h g^{-1} was achieved at 100 mA g^{-1}, exceeding the theoretical capacity and showing that significant secondary processes including electrode interface formation are contributing to the reduction charge. On reoxidation the observed capacities were 949 mA h g^{-1} at 200 mA g^{-1} and 1556 mA h g^{-1} at 100 mA g^{-1}, with first cycle Coulombic efficiencies of 64% and 60%, respectively. Both the reduction and oxidation processes contain a noteworthy plateau in the voltage profiles at around 0.3 V. From the second cycle efficiencies close top 100% were obtained, but the capacity at either rate gradually dropped to a value close to zero over the first 50 cycles. Some material was seen to drop off of the electrodes during cycling, and it is likely that the known problem of volume change during the tin alloying/dealloying processes are contributing to the capacity loss through mechanical damage to

the electrode composite films. Baggeto *et al* observed similar capacity losses from thin film electrodes, but were able to extend the lifetime of the electrodes by limiting the potential range over which they cycled.[29]

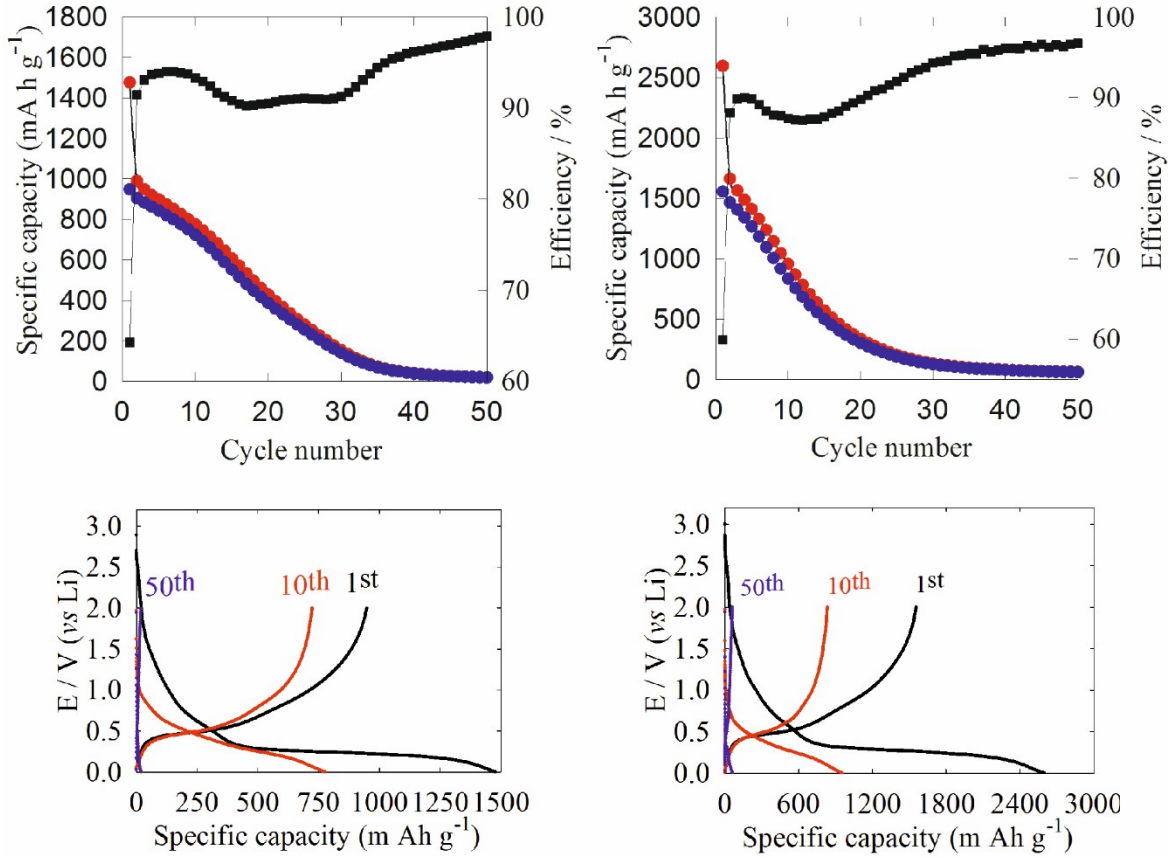

Fig. 6 Specific capacity versus cycle number (top, reduction blue, oxidation red and Coulombic efficiency black) and voltage profile against specific capacity (bottom), of Sn_3N_4/lithium half cells made with sodium alginate binder, cycled between 1 mV and 2 V for 50 cycles at 200 (left) or 100 (right) mA g^{-1}.

In order to understand the charge storage mechanism of Sn_3N_4 in Li half-cells, *ex situ* XRD data were collected (Fig. 7). Reduction to a voltage of 0.5 V, just above the large voltage plateau in the reduction profile in Fig. 5, showed reflections due to Sn_3N_4 and the copper substrate. Weak reflections due to tin metal were also observed. Similarly to the sodium cells the Sn_3N_4 reflections were weakened relative to the copper ones, but it is clear that the conversion reaction of Sn_3N_4 to Sn was incomplete before the plateau. On further reduction to 1 mV, the diffraction pattern showed only amorphous material, as previously observed in Li half-cells with tin electrodes.[48] On oxidising back to 2 V, broad reflections of Sn were observed in the XRD pattern but in contrast with the sodium cells Sn_3N_4 was not regenerated. Whilst some reformation of an amorphous nitride phase cannot be ruled out, this suggests that most of the reversible charge storage in this system is associated with tin alloying and de-alloying as previously suggested by Park *et al*.[28] The reformation

of Sn_3N_4 on oxidation in sodium cells but not in lithium cells may be related to the difference in stability of Li_3N (ΔH_f = -165 kJ mol^{-1})[49] compared with Na_3N ($\Delta H_f \approx$ +64 kJ mol^{-1}).[50]

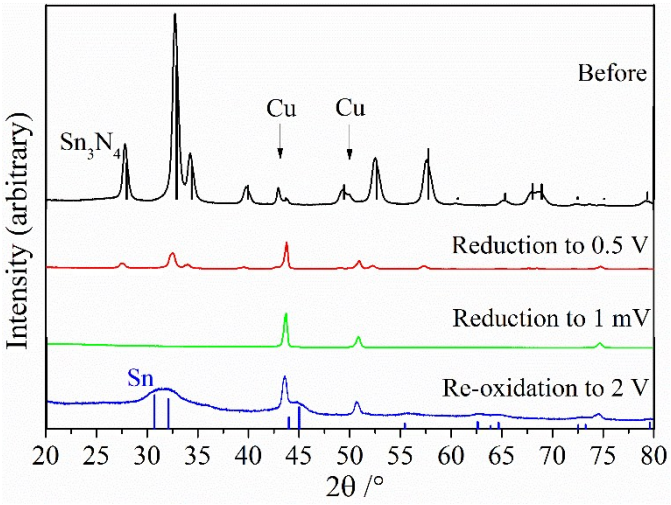

Fig. 7 *Ex situ* XRD of Sn_3N_4 electrodes cycled at 100 mA g^{-1} to different stages in lithium half cells. The black stick pattern denotes the literature positions and intensities of Sn_3N_4 reflections,[9] the main copper substrate peaks are labelled[47] and the positions of tetragonal tin reflections are marked with a blue stick pattern.[47]

Effect of addition of FEC on behaviour of Sn_3N_4 in lithium and sodium half cells

Fluoroethylene carbonate (FEC) is a well-known electrolyte additive that can improve the cycling performance of lithium batteries.[51,52,53] It was also found to improve the performance of Na-ion cells using hard carbon,[54] tin,[55] or antimony[56] as the negative electrode. It can aid the formation of compact solid electrolyte interface (SEI) films that can sometimes better withstand volume changes during cycling.

The effect of FEC on the performance of Sn_3N_4 in sodium and lithium half cells was investigated by replacing 5% of the solvent in the electrolytes used above with FEC and cycling cells in the same way. In both cases this led to an improvement in the specific capacities, and in the lithium cells it also led to an improvement in the cell stability (Fig. 8). In the sodium cell 680 mA h g^{-1} charge was passed in the first reduction, 35% of which (240 mA h g^{-1}) was recovered on re-oxidation. In contrast to the cells without FEC (Fig. 3) the Coulombic efficiency climbed gradually but was only ~95% after 50 cycles. However, the capacity after 50 cycles (270 mA h g^{-1}) is 35% higher than that of a cell without FEC cycled under the same conditions. A lithium cell prepared with the FEC additive (Fig. 8) exhibited similar reduction capacity in the first cycle at 200 mA g^{-1} (1540 mA h g^{-1}) to that without FEC (Fig. 6). The reduction capacity of the cell with FEC dropped more rapidly, to approximately 620 mA h g^{-1} in the 10th cycle, than that without. However, the cell with FEC stabilised in the subsequent cycles, whereas the cell without FEC underwent rapid capacity decay. In the 50th cycle, the cell prepared

using the FEC additive retained a capacity of around 370 mA h g^{-1} (60% of that in the 10th cycle). The cell without FEC had only 20 mA h g^{-1} (2.5% retention of the 10th cycle capacity).

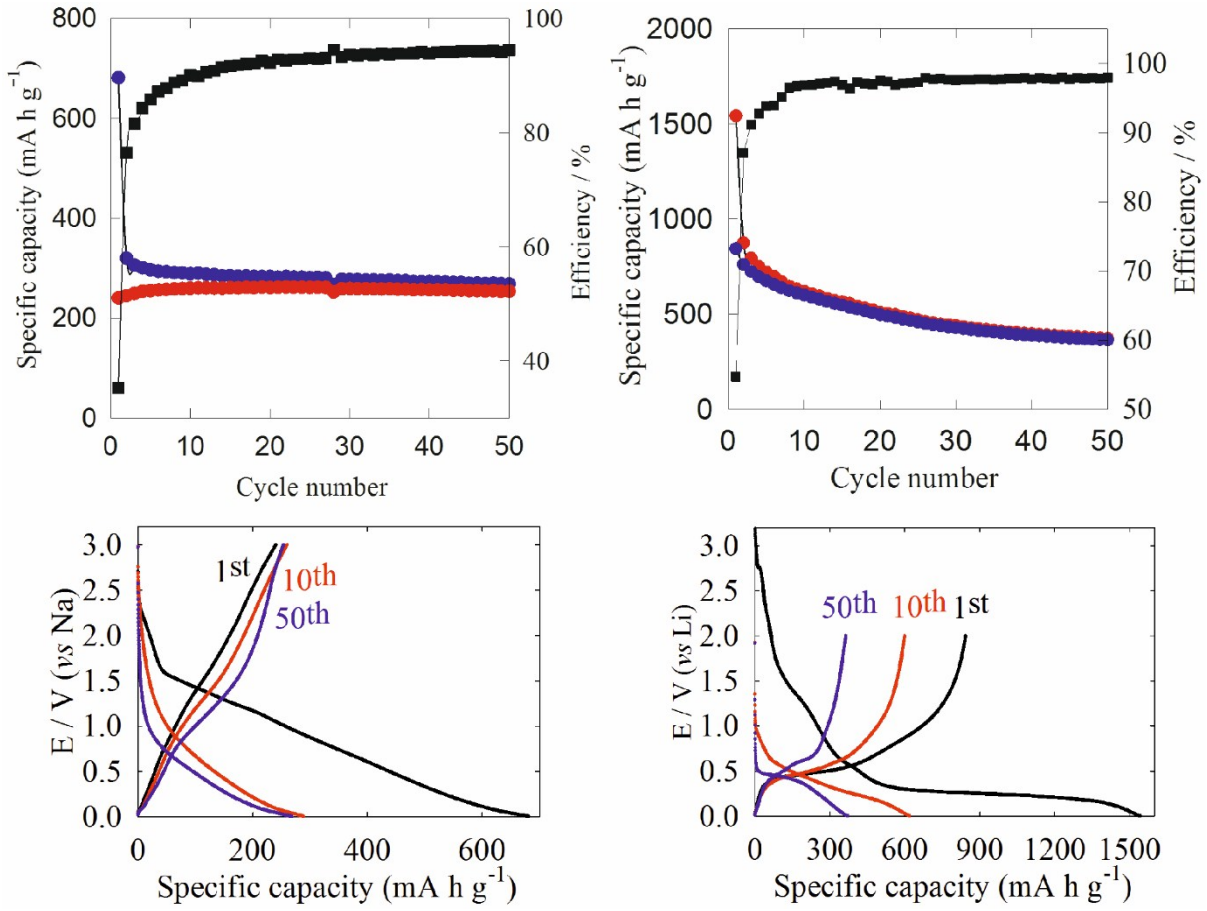

Fig. 8 Specific capacity versus cycle number (top, reduction blue, oxidation red and Coulombic efficiency black) and voltage profile against specific capacity (bottom), of a Sn_3N_4/sodium half cell cycled between 1 mV and 3 V for 50 cycles at 50 mA g^{-1} (left) or a Sn_3N_4/lithium half cell cycled between 1 mV and 2 V for 50 cycles at 200 mA g^{-1} (right).

Whilst FEC additions have proven effective in improving the performance of Sn_3N_4 in lithium and sodium cells, it is possible that a more radical change of electrolyte may offer further improvements. Carbonate-based electrolytes have been optimised for cells containing oxide materials with alkali metals or carbon, but nitride surfaces are more basic and may degrade the carbonate solvents more strongly. Hence further work will explore alternatives such as ionic liquids with quaternary ammonium cations.

Conclusions

Two step ammonolysis of $Sn(NEt_2)_4$ followed by washing with dilute acid is an effective route to tin(IV) nitride. The resultant nanocrystalline Sn_3N_4 powders showed good capacities in lithium cells, though with only moderate stabilities based mainly on alloying of the tin produced in the first

reduction of Sn_3N_4. In sodium cells reoxidation to Sn_3N_4 does occur and good capacities and stability are found, albeit lower capacities than with lithium. In both cell types the oxidation/reduction potentials are relatively low and these are mainly useful as negative electrodes. Carboxymethyl cellulose and sodium alginate binders worked well in these cells, with the latter giving superior cycling properties. These could also be improved by the addition of fluoroethylene carbonate to the electrolyte mixture. Employing these measures a capacity of 270 mA h g^{-1} was achieved in the 50th cycle of a sodium cell, and 370 mA h g^{-1} in the 50th cycle of a lithium cell.

Acknowledgements

The authors thank EPSRC for funding the Smartlab diffractometer under EP/K00509X/1 and EP/K009877/1, and acknowledge the use of the EPSRC-funded National Chemical Database Service hosted by the Royal Society of Chemistry.

References

[1] *Web of Science* database search, Thompson-Reuters, 2016.
[2] M. D. Slater, D. Kim, E. Lee and C. S. Johnson, *Adv. Funct. Mater.*, 2013, **23**, 947-958.
[3] P. Thomas, J. Ghanbaja and D. Billaud, *Electrochim. Acta*, 1999, **45**, 423-430.
[4] L. P. Wang, L. Yu, X. Wang, M. Srinivasan and Z. J. Xu, *J. Mater. Chem. A*, 2015, **3**, 9353-9378.
[5] X. Li, M. M. Hasan, A. L. Hector and J. R. Owen, *J. Mater. Chem. A*, 2013, **1**, 6441-6445.
[6] X. Li, A. L. Hector and J. R. Owen, *J. Phys. Chem. C*, 2014, **118**, 29568-29573.
[7] S. I. U. Shah, A. L. Hector, X. Li and J. R. Owen, *J. Mater. Chem. A*, 2015, **3**, 3612-3619.
[8] Z. Cui, C. Li, P. Yu, M. Yang, X. Guo and C. Yin, *J. Mater. Chem. A*, 2015, **3**, 509-514.
[9] N. Scotti, W. Kockelmann, J. Senker, S. Traβel and H. Jacobs, *Z. Anorg. Allg. Chem.*, 1999, **625**, 1435-1439.
[10] F. Fischer and G. Iliovici, *Ber. Deut. Chem. Ges.*, 1909, **42**, 527-537.
[11] L. Maya, *Inorg. Chem.*, 1992, **31**, 1958-1960.
[12] R. G. Gordon, D. M. Hoffman and U. Riaz, *Chem. Mater.*, 1992, **4**, 68-71.
[13] J. C. Remy and J. J. Hantzpergue, *Thin Solid Films*, 1975, **30**, 197-204.
[14] R. S. Lima, P. H. Dionisio and W. H. Schreiner, *Sol. St. Commun.*, 1991, 79, 395-398.
[15] N. Takahashi, K. Terada, T. Takahashi, T. Nakamura, W. Inami and Y. Kawata, *J. Elect. Mater.*, 2003, **32**, 268-271.
[16] M. P. Shemkunas, G. H. Wolf, K. Leinenweber and W. T. Petuskey, *J. Am. Ceram. Soc.*, 2002, **85**, 101-104.
[17] D. Y. W. Yu, P. V. Prikhodchenko, C. W. Mason, S. K. Batabyal, J. Gun, S. Sladkevich, A. G. Medvedev and O. Lev, *Nature Commun.*, 2013, **4**, 2922 (7 pages).
[18] L. Wu, H. Lu, L. Xiao, J. Qian, X. Ai, H. Yang and Y. Cao, *J. Mater. Chem. A*, 2014, **2**, 16424-16428.
[19] Y. C. Lu, C. Ma, J. Alvarado, N. Dimov, Y. S. Meng and S. Okada, *J. Mater. Chem. A*, 2015, **3**, 16971-16977.
[20] B. Qu, C. Ma, G. Ji, C. Xu, J. Xu, Y. S. Meng, T. Wang and J. Y. Lee, *Adv. Mater.*, 2014, **26**, 3854-3859.
[21] Y. Kim, Y. Kim, A. Choi, S. Woo, D. Mok, N.-S. Choi, Y. S. Jung, J. H. Ryu, S. M. Oh and K. T. Lee, *Adv. Mater.*, 2014, **26**, 4139-4144.
[22] J. Qian, Y. Xiong, Y. Cao, X. Ai and H. Yang, *Nano Lett.*, 2014, **14**, 1865-1869.
[23] J. Y. Jang, Y. Lee, Y. Kim, J. Lee, S.-M. Lee, K. T. Lee and N.-S. Choi, *J. Mater. Chem. A*, 2015, **3**, 8332-8338.
[24] D. Su, H.-Y. Ahn and G. Wang, *Chem. Commun.*, 2013, **49**, 3131-3133.
[25] Y. Wang, D. Su, C. Wang and G. Wang, *Electrochem. Commun.*, 2013, **29**, 8-11.
[26] Y.-X. Wang, Y.-G. Lim, M.-S. Park, S.-L. Chou, J. H. Kim, H.-K. Liu, S.-X. Dou and Y.-J. Kim., *J. Mater. Chem. A*, 2014, **2**, 529-534.
[27] I. A. Courtney and J. R. Dahn, *J. Electrochem. Soc.*, 1997, **144**, 2045-2052.
[28] K. S. Park, Y. J. Park, M. K. Kim, J. T. Son, H. G. Kim and S. J. Kim, *J. Power Sources*, 2001, **103**, 67-71.

[29] L. Baggetto, N. A. M. Verhaegh, R. A. H. Niessen, F. Roozeboom, J.-C. Jumas and P. H. L. Notten, *J. Electrochem. Soc.*, 2010, **157**, A340-A347.
[30] I. M. Thomas, *Can. J. Chem.*, 1961, **39**, 1386-1388.
[31] J. Lorberth, *J. Organomet. Chem.*, 1969, **16**, 235-248.
[32] A. C. Larson and R. B. Von Dreele, Generalized Structure Analysis System (GSAS), Los Alamos National Laboratory Report LAUR (2004) 86-748; B. H. Toby, *J. Appl. Cryst.*, 2001, **34**, 210-213.
[33] R. B. Von Dreele, A. C. Larson, GSAS manual, LANSCE MS-H805, Los Alamos National Laboratory, NM87545 (2000).
[34] S. Brunauer, P. H. Emmett and E. Teller, *J. Amer. Chem. Soc.*, 1938, **60**, 309-319.
[35] G. M. Brown and L. Maya, *J. Am. Ceram. Soc*., 1988, **71**, 78.
[36] D. V. Baxter, M. H. Chisholm, G. J. Gama, V. F. Distasi, A. L. Hector and I. P. Parkin, *Chem. Mater*., 1996, **8**, 1222-1228.
[37] A. W. Jackson, O. Shebanova, A. L Hector and P. F. McMillan, *J. Solid State Chem.*, 2006, **179**, 1383-1393.
[38] E. Bailey, N. M. T. Ray, A. L. Hector, P. Crozier, W. T. Petuskey and P. F. McMillan, *Materials*, 2011, **4**, 1747-1762.
[39] A. Salamat, A. L. Hector, B. M. Gray, S. A. J. Kimber, P. Bouvier and P. F. McMillan, *J. Am. Chem. Soc.*, 2013, **135**, 9503-9511.
[40] A. Salamat, K. Woodhead, S. I. U. Shah, A. L. Hector and P. F. McMillan, *Chem. Commun.*, 2014, **50**, 10041-10044.
[41] S. I. U. Shah, A. L. Hector and J. R. Owen, *J. Power Sources*, 2014, **266**, 456-463.
[42] B. Lestriez, S. Bahri, I. Sandu, L. Roué and D. Guyomard, *Electrochem. Commun.*, 2007, **9**, 2801-2806; N. S. Hochgatterer, M. R. Schweiger, S. Koller, P. R. Raimann, T. Wöhrle, C. Wurm and M. Winter, *Electrochem. Solid-State Lett.*, 2008, **11**, A76-A78; D. Mazouzi, B. Lestriez, L. Roué and D. Guyomard, *Electrochem. Solid-State Lett.*, 2009, **12**, A215-A218; J. S. Bridel, T. Azaïs, M. Morcrette, J. M. Tarascon and D. Larcher, *Chem. Mater.*, 2010, **22**, 1229-1241.
[43] S.-L. Chou, X.-W. Gao, J.-Z. Wang, D. Wexler, Z.-X. Wang, L.-Q. Chen and H.-K. Liu, *Dalton Trans.*, 2011, **40**, 12801-12807.
[44] J. Li, H. M. Dahn, L. J. Krause, D.-B. Le and J. R. Dahn, *J. Electrochem. Soc.*, 2008, **155**, A812-A816.
[45] I. Kovalenko, B. Zdyrko, A. Magasinski, B. Hertzberg, Z. Milicev, R. Burtovyy, I. Luzinov and G. Yushin, *Science*, 2011, **334**, 75-79
[46] P. S. Veluri and S. Mitra, *RSC Adv.*, 2013, **3**, 15132-15138.
[47] *Inorganic Crystal Structure Database* (Fiz Karlsruhe) accessed via the *National Chemical Database Service* hosted by the Royal Society of Chemistry.
[48] H. S. Im, Y. J. Cho, Y. R. Lim, C. S. Jung, D. M. Jang, J. Park, H. Shojaei and H. S. Kang, *ACS Nano*, 2013, **7**, 11103-11111.
[49] P.A.G. O'Hare and G. K. Johnson, *J. Chem. Thermodyn.*, 1975, **7**, 13-20.
[50] G. V. Vajenine, *Inorg. Chem.*, 2007, **46**, 5146-5148.
[51] H. Nakaiz, T. Kubota, A. Kita and A. Kawashima, *J. Electrochem. Soc.*, 2011, **158**, A798-A801.
[52] R. Mogi, M. Inaba, S.-K. Jeong, Y. Iriyama, T. Abe and Z. Ogumi, *J. Electrochem. Soc.*, 2002, **149**, A1578-A1583.
[53] R. McMillan, H. Slegr, Z. X. Shu and W. Wang, *J. Power Sources*, 1999, **81-82**, 20-26.
[54] S. Komaba, T. Ishikawa, N. Yabuuchi, W. Murata, A. Ito, and Y. Ohsawa, *ACS Appl. Mater. Interfaces*, 2011, **3**, 4165-4168.
[55] S. Komaba, Y. Matsuura, T. Ishikawa, N. Yabuuchi, W. Murata and S. Kuze, *Electrochem. Commun.*, 2012, **21**, 65-68.
[56] J. Qian, Y. Chen, L. Wu, Y. Cao, X. Ai and H. Yang, *Chem. Commun.*, 2012, **48**, 7070-7072.

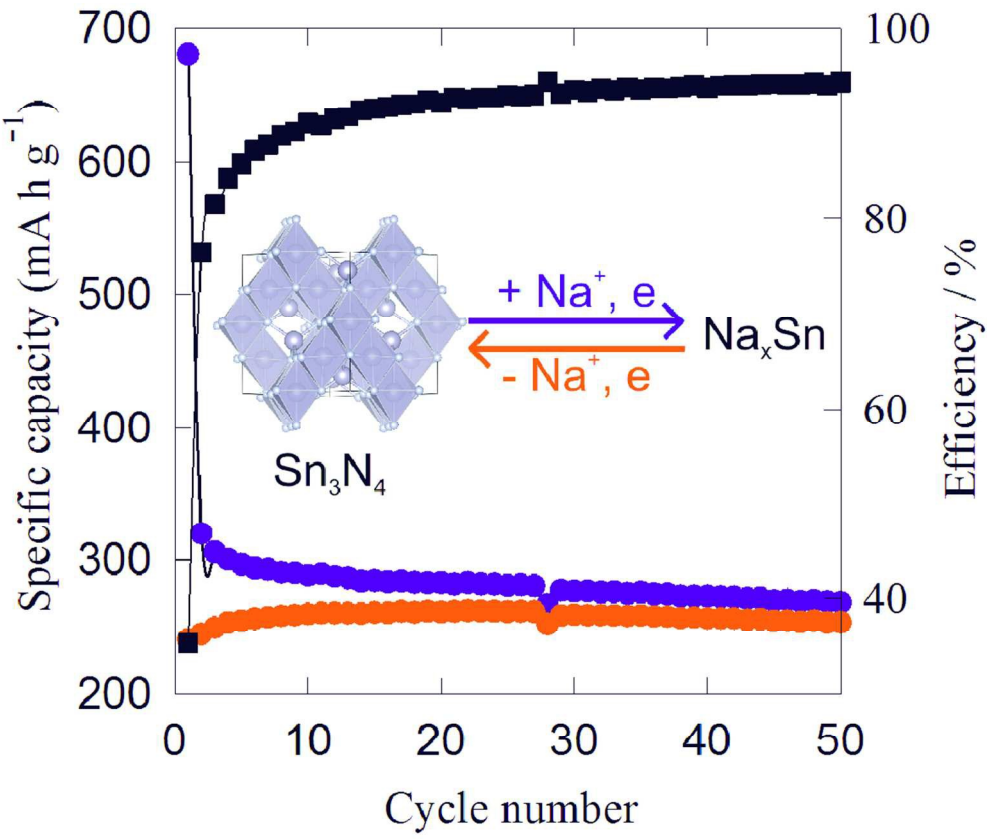

99x83mm (300 x 300 DPI)